Response to Reviewer #3

Comment: *This study focuses on the impact of primarily emitted oxygenated volatile organic compounds (OVOCs) on ozone formation in the Yangtze River Delta region. By integrating an updated anthropogenic emission inventory with source-resolved profiles and the CMAQ model, it optimizes the simulation of OVOCs in the region. Combined with observational data from spring and autumn 2019, the study systematically analyzes the spatiotemporal distribution, source characteristics of OVOCs and their role in the ozone formation chain. The research is solid with sufficient data support, filling the research gap in the region and providing important scientific basis for targeted ozone pollution control with clear practical guiding significance. While the paper demonstrates a clear structure and standardized methods that meet journal publication requirements, it requires further revisions before being recommended for acceptance.*

Response: We sincerely thank the reviewer for the positive and constructive feedback on our study. These comments have substantially improved the clarity, rigor, and overall quality of the manuscript. In response to the reviewer's suggestions, we have: (1) added sensitivity simulations for primary OVOCs emitted from industrial processes, solvent use, transportation, and residential sources to quantify their impacts on ozone production rates as well as HO_2 and RO_2 radical concentrations; (2) conducted additional simulations incorporating temperature-dependent adjustments of evaporative emissions to assess the influences on OVOC levels; (3) quantified the contributions of OVOCs to primary HO_2, RO_2, and RO_x production; (4) elaborated on the heterogeneous and nonlinear responses of ozone to changes in OVOC emissions; (5) refined the description of observational data processing; and (6) made revisions to improve the clarity of the text and to standardize the fonts in all figures. Detailed responses to each comment are provided below. The reviewer's comments are shown in black italics, our responses are provided in blue, and the corresponding revisions in the manuscript are highlighted in red.

General Comments:

Comment: *It is recommended that the authors strengthen the analysis of the synergistic effects between primary OVOC emissions and other key pollutants (e.g., NO_x, CO, and traditional VOCs) across different source sectors. The study has well quantified the individual contributions of OVOCs to ozone formation, but it lacks in-depth discussion on how the interactions between OVOCs from specific sources (e.g., industrial processes, solvent use, and transportation) and other pollutants regulate the radical budget (especially HO_2 and RO_2) and ozone production efficiency. For instance, the differential impacts of OVOC-sourced HO_2 radicals on NO-to-NO_2 conversion under*

varying NO_x levels (high-NO_x urban areas vs. low-NO_x suburban areas) are not fully elaborated. It is suggested to supplement comparative analysis of such synergistic mechanisms, combined with source-resolved sensitivity simulations, to clarify the context-dependent roles of primary OVOCs in ozone formation, thereby enhancing the practical relevance for targeted emission control strategies.

Response: Thank you for the insightful suggestions. We have conducted four additional sensitivity simulations to assess the impacts of primary OVOCs emitted from industrial processes, solvent use, transportation, and residential sources in the YRD region on daytime peroxy radical (HO_2 and RO_2) concentrations and ozone production rates ($P(O_3)$) (Figs. R1-R4). In these simulations, OVOC emissions from each source category were individually set to zero. Among these sources, industrial processes showed the strongest impacts in Jiangsu Province, contributing up to 4 ppb h^{-1} of $P(O_3)$ and more than 1 ppt to HO_2 and RO_2 concentrations. The impacts of solvent use were mainly concentrated in the adjacent areas of Shanghai, Jiangsu, and Zhejiang, contributing up to 1 ppb h^{-1} to $P(O_3)$ and up to 36.8% of HO_2 and 46.8% of RO_2 radicals. For residential sources, the impacts on $P(O_3)$ were mainly concentrated in the central and northern YRD, with a hotspot over Shanghai reaching more than 0.1 ppb h^{-1}. In contrast, their influence on peroxy radicals was more spatially widespread across the YRD, contributing up to 2% of HO_2 and 3% of RO_2. Transportation sources exhibited relatively small but spatially widespread impacts on $P(O_3)$ as well as on HO_2 and RO_2, contributing up to 5.2%, 5.7%, and 4.0%, respectively. Overall, all these source categories except residential sources showed stronger impacts on HO_2 than RO_2 in regions strongly affected by anthropogenic emissions, highlighting the important role of primary OVOCs in ozone formation via the HO_2 + NO pathway.

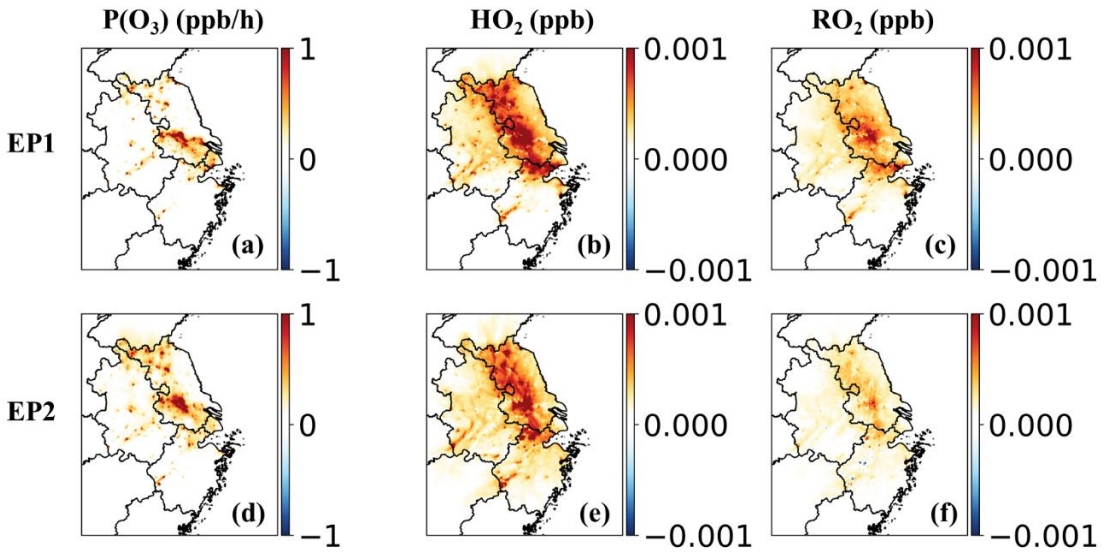

Figure R1. Contributions of OVOCs emitted from industrial processes to the daytime ozone production rate ($P(O_3)$, ppb h^{-1}) and HO_2 and RO_2 radical concentrations (ppb) during EP1 and EP2. The contributions are quantified as the differences between the base case and a sensitivity case in which

OVOC emissions from the corresponding sources are set to zero.

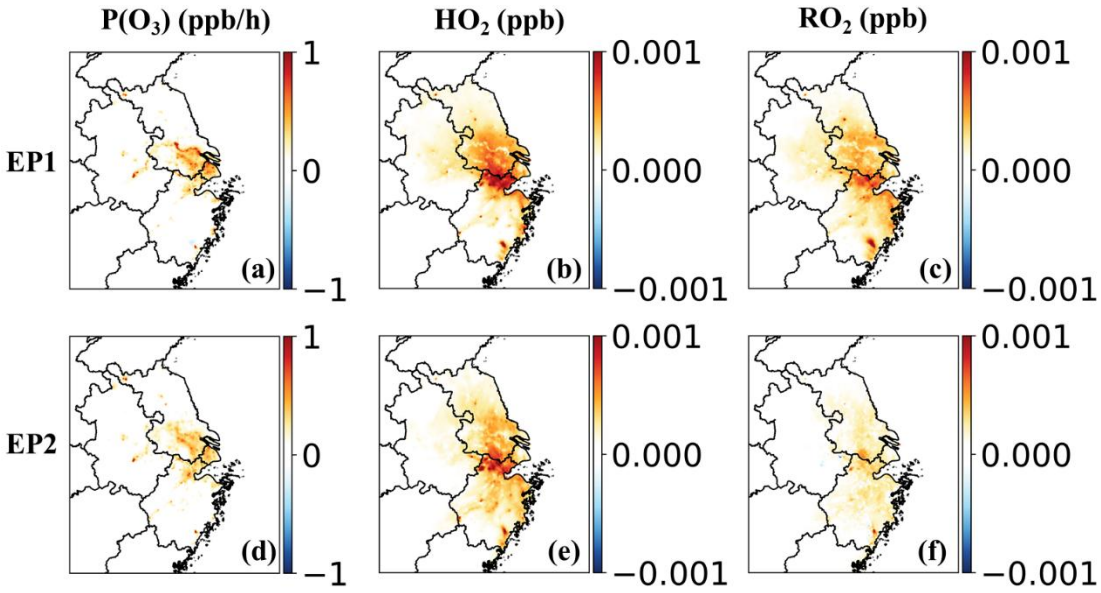

Figure R2. Same as Figure R1 but for the impacts of OVOCs emitted from solvent use sources.

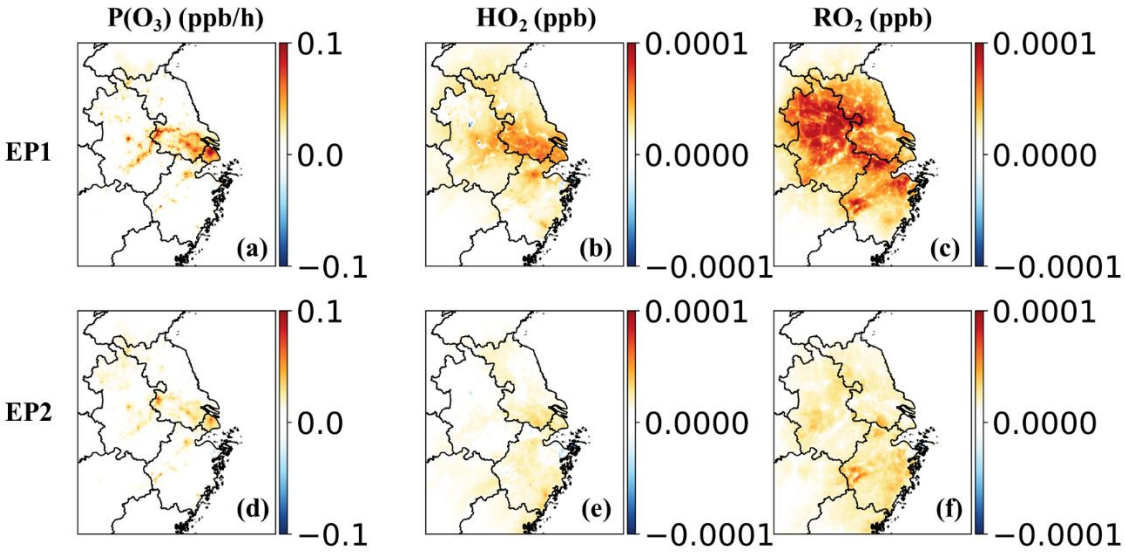

Figure R3. Same as Figure R1 but for the impacts of OVOCs emitted from residential sources.

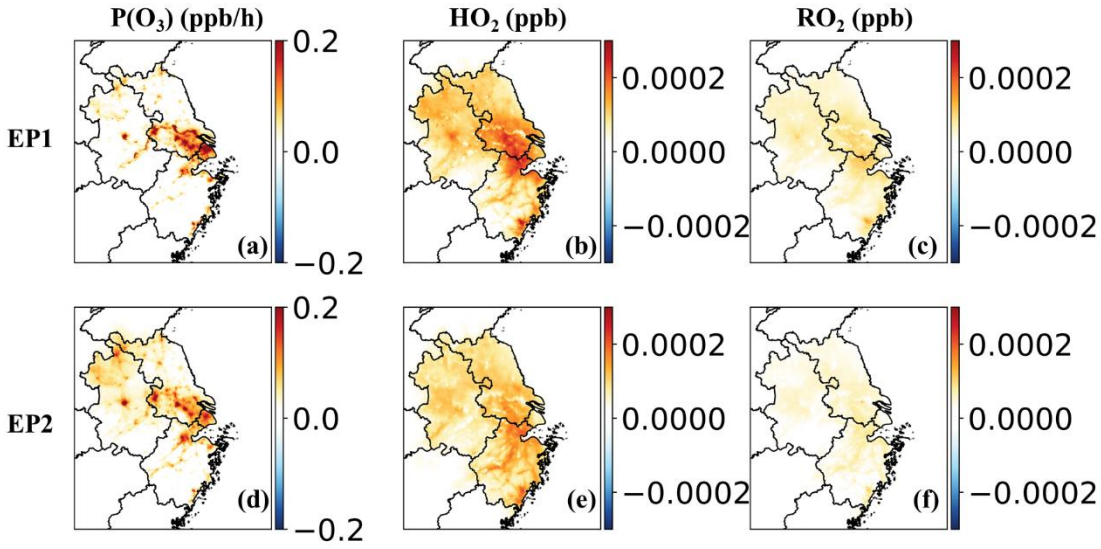

Figure R4. Same as Fig. R1 but for the impacts of OVOCs emitted from transportation sources.

Based on the daytime $P(O_3)$ attributable to HO_2-driven NO-to-NO_2 conversion (Fig. 4), higher contributions were observed in the northern YRD, coinciding with elevated NO_x emission rates (approximately 0.4−2.0 mole s^{-1}; Fig. R5). In these regions, the more pronounced influence of HO_2 compared to RO_2 on $P(O_3)$ is primarily associated with markedly higher HO_2 concentrations. OVOCs dominated primary HO_2 production (>90%) in this region, with primary OVOCs alone contributing approximately 20−50% (Fig. 4). In addition, OVOCs contributed approximately 50−98% of primary RO_2 and 40−70% of primary RO_x production, suggesting that OVOCs also play an important role in sustaining HO_2 levels through radical cycling. Taken together, the pronounced influence of HO_2 on $P(O_3)$ in urban regions is likely driven by elevated levels of both primary OVOCs and secondary OVOCs formed from VOC oxidation. Such conditions, characterized by coexisting high emissions of reactive organic gases and NO_x, are conducive to enhanced HO_2 production. We have added a discussion in the revised manuscript as follows:

Lines 311-322: "The dominant role of HO_2-driven oxidation in ozone production was further confirmed in other urban areas of the YRD. During both EP1 and EP2, HO_2 radicals contributed approximately 55−80% of total ozone production in regions with elevated $P(O_3)$ (Figs. 4a, d and S11a, d). These regions, including Shanghai, are strongly affected by anthropogenic emissions, with substantial NO_x emission rates (approximately 0.4−2.0 mole s^{-1}; Fig. S9) and HO_2 concentrations exceeding those of RO_2 radicals (Fig. S11). In these urban areas, primary OVOCs from major sources, such as industrial processes, solvent use, residential sources, and transportation, made substantial contributions to $P(O_3)$ and peroxy radical levels (particularly HO_2), ranging 5−40% and 4−47%, respectively (Figs. S12−S15). In contrast, the RO_2 pathway dominated ozone production in the southern and southwestern parts of the domain,

where high emissions of biogenic VOCs and relatively low emissions of NO_x prevail (Fig. S9). The enhanced role of RO_2 radicals in these regions is attributed to their higher concentrations and comparable reactivities to HO_2 radicals in converting NO to NO_2."

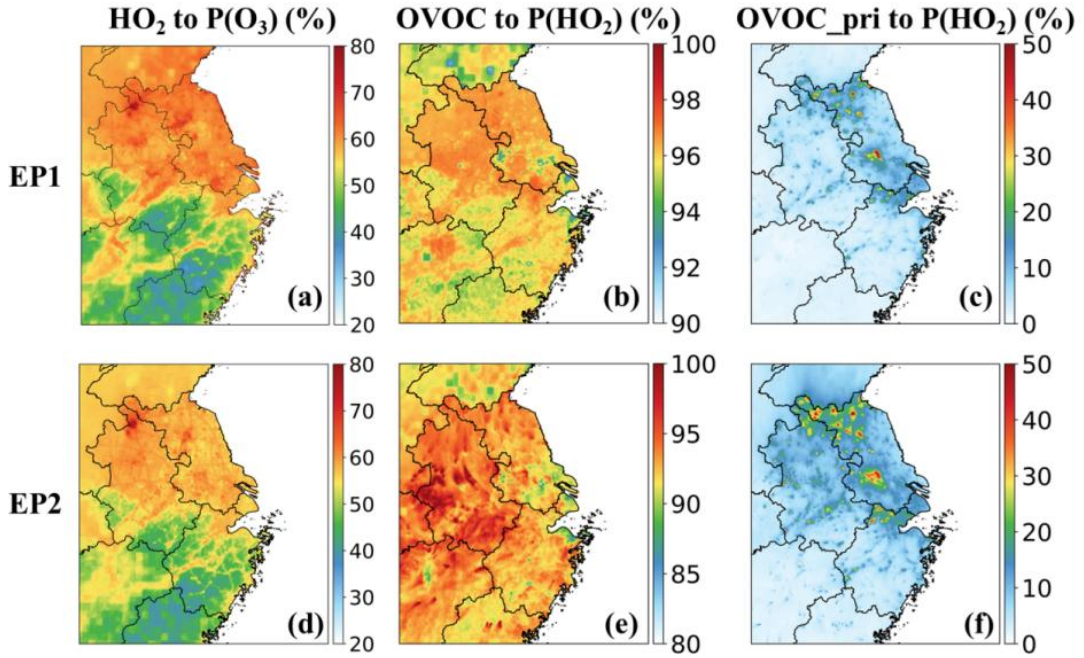

Figure 4. Daytime-averaged contributions of the HO_2 + NO pathway to ozone production rates (a, d), OVOC contributions to primary HO_2 radical production (b, e), and contributions from primary OVOCs (c, f) during the two episodes.

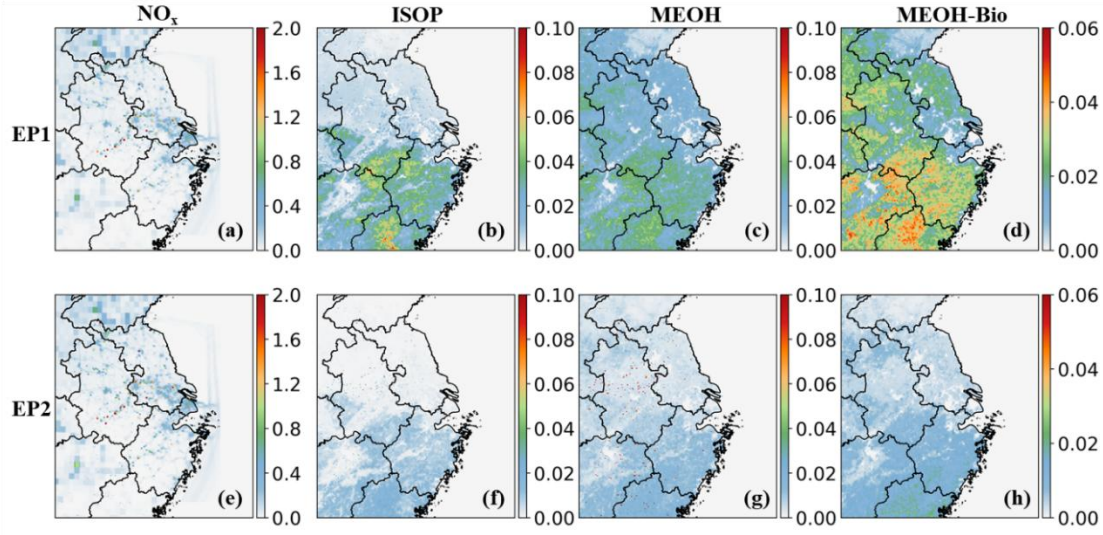

Figure R5. Average emission rates of NO_x, isoprene, MEOH, and biogenic MEOH during EP1 and EP2. Units are mole s^{-1}.

Specific Comments:

Comment: *1. Line 150. The study mentions that emissions of highly volatile OVOCs such as ethanol are significantly affected by temperature, but the current model has not*

fully incorporated temperature-dependent parameterization. It is recommended to supplement the basis for the setting of temperature-related parameters in the existing emission inventory, or provide a sensitivity analysis to verify the degree of temperature's impact on the simulation results.

Response: Thank you for this valuable comment. In the current emission inventory, evaporative emissions (e.g., from solvent use and gasoline evaporation) are not explicitly parameterized as temperature-dependent. To assess the potential impacts, we conducted additional sensitivity simulations by applying temperature-dependent adjustments to solvent use and gasoline evaporative OVOC emissions, following the approach used in our previous study (Qin et al. 2025). The simulated concentrations of OVOCs, including ethanol (ETOH), acetone (ACET), and formaldehyde (HCHO), showed slight decreases during the warm season (EP1) and more pronounced reductions during the cold season (EP2) across the YRD region (Fig. R6).

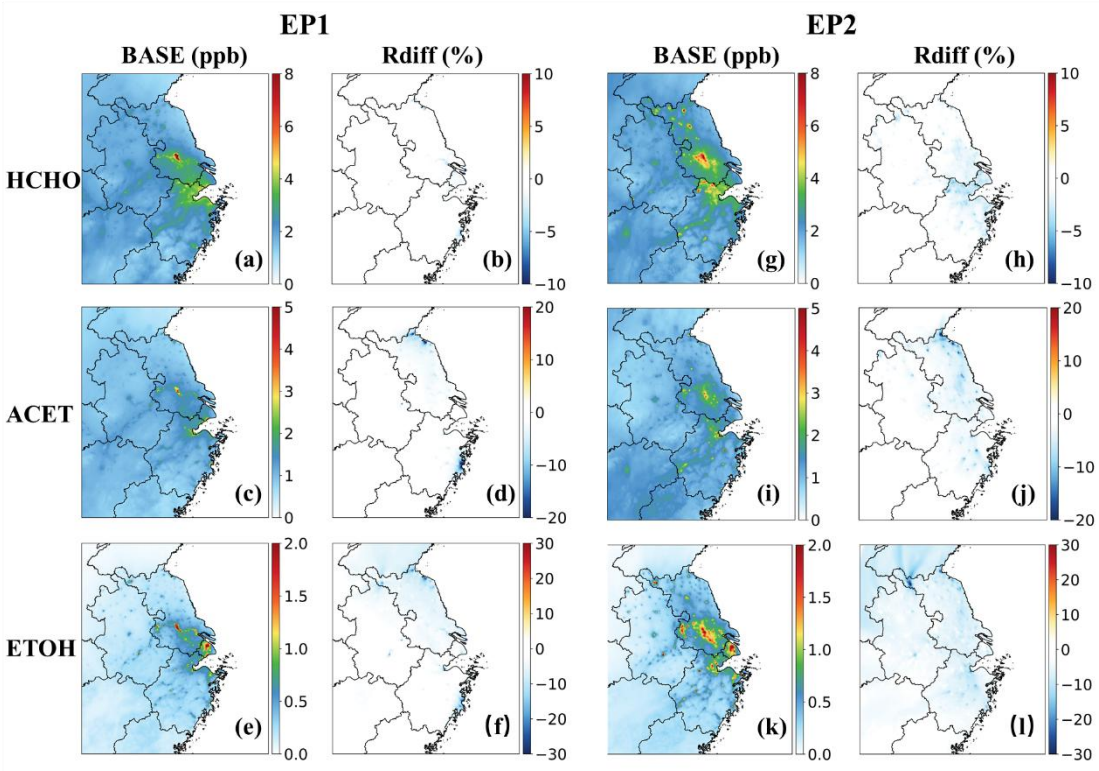

Figure R6. Episode averaged concentrations of HCHO, ACET, and ETOH in the base case (unit: ppb) and the relative changes due to temperature-adjusted evaporative emissions (Rdiff, (tempadj-base)/base %).

This is because the daily maximum surface temperature during both episodes, particularly in regions strongly influenced by anthropogenic emissions, was lower than the reference temperature (25 °C) used to scale evaporative emissions based on temperature-dependent emission factors. We acknowledge that this adjustment approach is still subject to uncertainties, including the choice of reference temperature and potential variability in temperature dependence among different volatile species

due to differences in vapor pressure. A more robust assessment of temperature-dependent evaporative emissions would require species-specific temperature-emission relationships from different sources, which is beyond the scope of the present study. To avoid confusion and potential misinterpretation, we have therefore removed the related discussion on the impacts of temperature-dependent evaporative emissions on OVOC simulations from the revised manuscript.

Comment: *2. Line 170. The model shows consistent underestimation of species such as formic acid and acetic acid, and seasonal differences in the simulation of acetone (ACET). In addition to the uncertainties in the emission inventory and missing secondary formation pathways mentioned in the paper, have the local source impacts of the observation site been considered? It is recommended to supplement a brief description of the pollution source distribution around the site.*

Response: Thank you for this suggestion. The monitoring site is strongly affected by emissions from transportation and solvent use. Correlation analysis for acetic acid with other measured species showed high correlations with ethyl acetate, methyl ethyl ketone (MEK), and toluene (Pearson coefficients of 0.75−0.85, $p < 0.001$) in both periods. These compounds are typically associated with emissions from volatile chemical products (VCPs), consistent with the significant impacts of solvent use at the site. Additionally, strong correlations between acetic acid and biomass burning tracers (e.g., guaiacol and furan compounds and their derivatives) were observed during EP2, indicating an influence of this source on acetic acid at the monitoring site. Inadequate representations of these emissions may lead to biases in the current model.

For ACET, a more pronounced model bias is observed in EP1 (warm season) than in EP2 (cold season). As biogenic emissions are an important source of ACET, this bias may be partially attributed to underestimated biogenic emissions from urban green spaces near the monitoring site as also reflected by the model biases in isoprene. We have incorporated the related discussion into the manuscript in Lines 199-205:

"During EP2, acetic acid exhibited strong correlations with biomass burning tracers, such as guaiacol and furan compounds and their derivatives (Pearson coefficients > 0.80, $p < 0.001$). In addition, acetic acid showed consistently high correlations with ethyl acetate, methyl ethyl ketone (MEK), and toluene (Pearson coefficients of 0.75−0.85, $p < 0.001$) in both periods, species that are commonly associated with emissions from volatile chemical products (VCPs) (Wang et al., 2024b; McDonald et al., 2018). The underestimation of emissions from these sources likely contributes to the low bias in simulated acetic acid concentrations."

Lines 234-237: "Model performance for ACET varied seasonally, with good agreement in EP2 but significant underestimation in EP1. Since biogenic sources of acetone are

important (Lyu et al., 2024; Hu et al., 2013), the larger discrepancy observed in the warm season may be partially due to the model's inadequate representation of urban green vegetation (Maison et al., 2024; Ma et al., 2022)."

A description of the local emission impacts on the observation site is provided in Lines 187-189:
"The monitoring site is located in a typical urban environment characterized by dense commercial and residential buildings and heavy traffic, with strong influences from transportation and solvent use emissions (Liu et al., 2019; Liu et al., 2021)."

Comment: *3. Section 3.2. Since RO_2, HO_2, and OH can interconvert through the RO_x radical cycle, and the contribution of RO_2 to $P(O_3)$ cannot be ignored, especially in northern Zhejiang Province. It is requested to provide the contributions of OVOCs to primary RO_x radicals and RO_2 radicals. Which OVOCs are relatively important in this process?*

Response: Thank you for this insightful comment. We agree with the reviewer that RO_2, HO_2, and OH radicals are closely correlated and interconvert through radical chemistry. Therefore, we focus on primary RO_2, HO_2, and RO_x production, which are defined as those generated only as products in the reactions, such as photolysis of OVOCs, O_3, HONO, and ozonolysis of OVOCs and VOCs (Figs. 3, 4, and S16). Primary radicals initiate atmospheric radical chemistry and trigger radical chain reactions, ultimately leading to ozone accumulation. By focusing on the contribution of OVOCs to primary radical production, we provide a clearer and more robust assessment of their role in ozone formation. The results show that OVOCs contribute 63.96% (66.49%) and 95.31% (97.03%) of primary RO_2 and HO_2 at the monitoring site during clean (polluted) periods. Formaldehyde (HCHO), photoreactive monounsaturated dicarbonyls from aromatic fragmentation (AFG1), methylglyoxal (MGLY), and glyoxal (GLY) are the major contributors to HO_2 radical. A significant fraction of RO_2 radicals is produced by biacetyl (BACL), AFG1, and MGLY. For RO_x radicals, 50.18% and 43.17% are attributed to OVOC photooxidation under clean and polluted conditions. At the regional scale, the contributions of OVOCs to primary HO_2, RO_2, and RO_x radicals can reach approximately 90−98%, 50−98%, and 40−70%, respectively. These findings indicate a dominant role of OVOCs in radical production in the YRD. We have revised the manuscript to include a discussion on the role of OVOCs on primary HO_2, RO_2, and RO_x production in Section 3.2 (now Section 3.3).

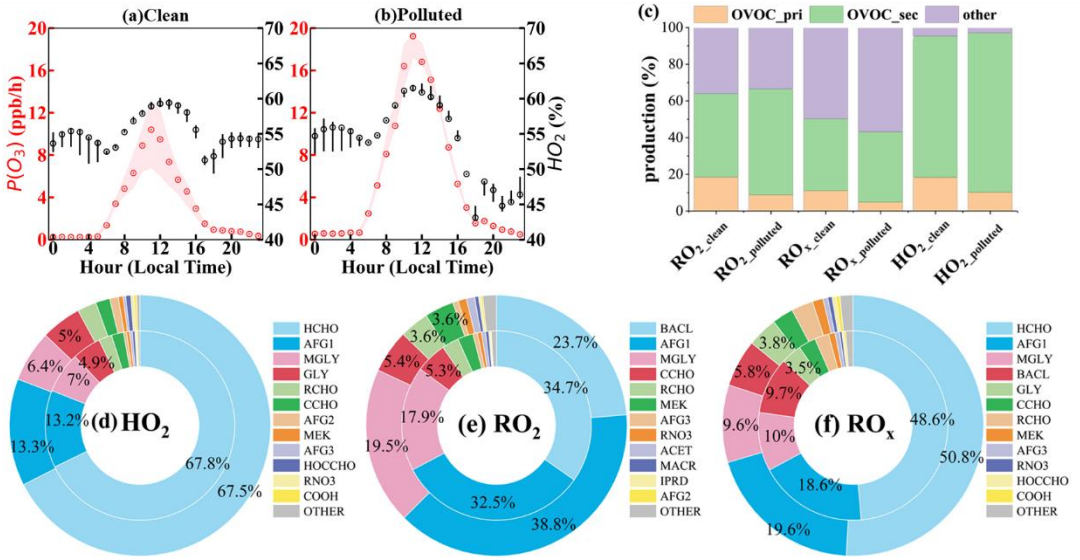

Figure 3. Diurnal variations of ozone production rates (a, b) and contributions of major sources (c) and individual OVOC species (d-f) to daytime primary HO_2, RO_2, and RO_x production under clean and polluted conditions at SAES in Shanghai. In panels (a) and (b), red and black circles represent the median $P(O_3)$ and the contribution of the HO_2 + NO pathway, respectively. The shaded areas and black error bars denote the interquartile ranges. In panel (c), "OVOC_pri" and "OVOC_sec" denote contributions from primary and secondary OVOCs, respectively. Panels (d-f) show the fractional contributions of individual OVOC species to total OVOC-derived primary radical productions during clean (inner ring) and polluted (outer ring) periods.

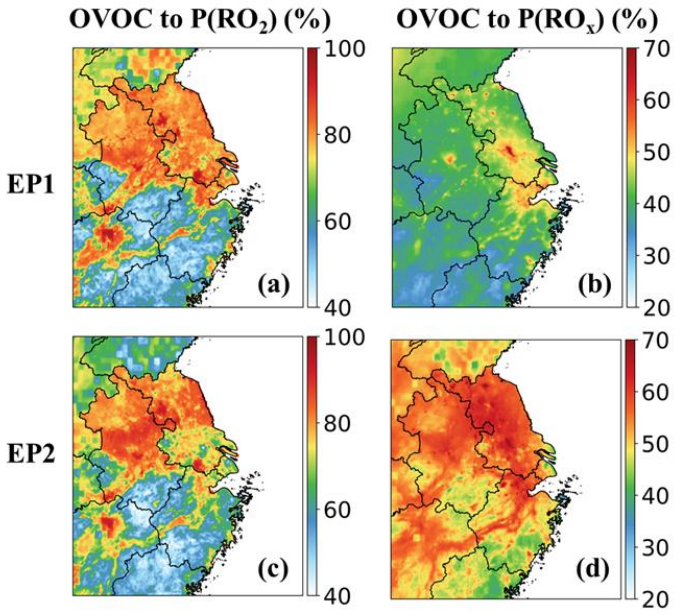

Figure S16. Contributions of OVOCs to the daytime primary RO_2 and RO_x radical production during EP1 and EP2.

Comment: *4. Section 3.3. When evaluating the sensitivity of ozone formation to OVOCs, explain why the emission reductions of some OVOCs lead to a nonlinear*

response of slight increases in ozone concentration, and whether this is related to the regional NO_x concentration levels? Will the experimental setup change NO_X? It is recommended to add relevant discussions in this section.

Response: Thank you for pointing out this phenomenon that requires an in-depth explanation. The High-Order Decoupled Direct Method (HDDM) calculates the spatially and temporally varying sensitivity coefficients of ozone changes to small perturbations in precursor emissions, i.e., the partial derivatives between the two. It can deal with the non-linear relationship between ozone and precursors by utilizing second-order (and higher) sensitivities, and compute ozone sensitivities to multiple precursors at once. In the current study, the first- and second-order sensitivity coefficients of each OVOC and VOC species are used to estimate ozone sensitivities to their emission changes, without altering NO_x emissions or concentrations.

The slight increase in ozone concentration observed in the simulation of emission reductions for certain OVOCs is likely related to their mechanisms in regulating NO_x and radical cycling. During the daytime, photooxidation of some aldehydes and ketones, such as acetaldehyde (CCHO), aromatic aldehydes (BALD), lumped C_3+ aldehydes (RCHO), and acrolein (ACRO), produces peroxyacyl radicals that can react with NO_2 to produce NO_x reservoir species, such as PAN and analogues. Reducing their emissions may therefore decrease PAN formation, allowing more NO_2 to remain available for NO_x cycling and thereby enhancing ozone production. At the same time, the photooxidation of CCHO, RCHO, and ACRO also produces other RO_2 and HO_2 radicals that promote NO-to-NO_2 conversion, implying that reductions in these OVOCs can partially suppress ozone formation by limiting peroxy radical production. Because the emission rates of these OVOCs, as well as the types and yields of radicals produced from their oxidation, vary substantially across the YRD, the net ozone response to their emission reductions exhibits spatial heterogeneity. Similarly, the products of CRES oxidation can either react with NO_2 to form relatively stable products or promote RO_2 and HO_2 productions, leading to regional differences in ozone responses to CRES emission reductions. We have added relevant discussions in the revised manuscript as follows:

Lines 404-410: "Notably, emission reductions of certain OVOCs (e.g., CCHO, RCHO, ACRO, and CRES) can lead to spatially divergent ozone responses, with both increases and decreases in the YRD. This likely arises from differences in the radical pathways associated with OVOC photooxidation: some pathways involve reactions with NO_2 to form relatively stable NO_x reservoir species, whereas others promote NO-to-NO_2 conversion. The competition between these pathways varies regionally with the abundances of OVOCs and NO_x, resulting in spatial heterogeneity in ozone sensitivities."

Comment: *5. Line 127. Since PTR can only measure the total molecular signal, how to process its measured data to distinguish the concentration of specific OVOCs? Alcohols produce fragments during proton transfer reactions, such as (C2H6OH+H+ → C2H4H++H2O). How to handle the concentration of alcohols measured by PTR?*

How is the quantification of OVOCs done? Can you supplement the comparison of two MSs?

Response: Thank you for this important comment that helps enhance the validity of OVOC measurements. As noted by the reviewer, proton-transfer-reaction time-of-flight mass spectrometry (PTR-ToF-MS) is capable of resolving isobaric ions but remains intrinsically limited to molecular-level characterization and cannot unambiguously distinguish isomers. In this study, the molecular formula for individual mass spectral peaks was first constrained by jointly applying the elemental composition tool implemented in the Tofware software package v3.2.3 (Tofwerk Inc.), the PTR-MS spectral library (Pagonis et al., 2019), and the PubChem database. Based on these plausible molecular formulae, tentative compound identifications were further inferred by integrating previously reported source-specific emission profiles from the literature. For species quantification, sensitivities for species with authentic standards were determined through calibration using multi-gradient known concentrations of given VOCs. For identified species lacking standards, their theoretical sensitivities were estimated based on the correlations with kinetic rate constants of VOCs (Sekimoto et al., 2017). This approach has been successfully employed to identify reactive organic gases emitted from residential combustion in the YRD (Gao et al., 2022; 2023).

Alcohol compounds are prone to fragmentation during proton transfer reactions, such that the primary ion typically accounts for ~80% of the total ion signal, resulting in an approximate 20% underestimation of their concentrations. In the current study, small alcohols such as methanol and ethanol were detected using an online gas chromatography system equipped with a mass spectrometer and a flame ionization detector (GC-MS/FID). The results for major aromatic hydrocarbons and carbonyl compounds measured by PTR-QiTOF and GC-MS/FID showed good agreement, as illustrated in Fig. S5 of Gao et al (2022).

We have revised the manuscript with detailed information on the treatment of PTR-QiTOF measurements and comparison between PTR-QiTOF and GC-MS/FID as follows:

Lines 148-160: "High time-resolution measurements of 77 OVOCs, including 14 aldehydes and ketones, 23 organic acids and esters, 10 furan compounds, and 30 oxygenated aromatic compounds, were recorded at a 10s interval using a Proton

Transfer Reaction-Quadruple interface Time-of-Flight Mass Spectrometer (PTR-QiTOF) at the Shanghai Academy of Environmental Sciences (SAES). Species were identified by jointly applying the Tofware software package v3.2.3 (Tofwerk Inc.), the proton transfer reaction mass spectrometry (PTR-MS) spectral library (Pagonis et al., 2019), the PubChem database, and source-specific emission profiles reported in literature (Hatch et al., 2017; Koss et al., 2018; Stockwell et al., 2021; Tanzer-Gruener et al., 2022; Coggon et al., 2021). Sensitivities for species with authentic standards were determined through calibration using multi-gradient known concentrations of given VOCs. For identified species lacking standards, their theoretical sensitivities were estimated based on correlations with kinetic rate constants of VOCs (Sekimoto et al., 2017). The raw data were screened to remove outliers (values below background levels) and missing data, and then averaged to hourly means."

Lines 161-165: "In addition, C_2–C_{12} hydrocarbons, C_2–C_5 carbonyls, and C_1–C_4 alcohols were measured using an online gas chromatography system equipped with a mass spectrometer and a flame ionization detector (GC-MS/FID, TH-300, Wuhan Tianhong Instruments, China) at an hourly resolution. For major aromatic hydrocarbons and carbonyl compounds, good agreement between measurements by PTR-QiTOF and GC-MS/FID was observed (Gao et al., 2022)."

Comment: *6. With reference to Table S6, could the contribution ratios of different sources to each OVOC in EP1 and EP2 be provided separately?*
Response: Thank you for this suggestion. The current study mainly focuses on the implementation of a newly developed emission inventory to improve the simulations of OVOCs and assess their roles in ozone formation, particularly for that of primary OVOCs. The development of the inventory, including the source profiles of all the pollutants emitted from anthropogenic sectors, will be detailed in another manuscript.

Comment: *7. It is recommended that the fonts in the figures and tables be consistent.*
Response: We have reviewed and standardized the fonts across all figures (primarily using Times New Roman), ensuring consistency in size and style to meet the journal's figure formatting requirements.

Comment: *8. Fig. 1 (2) b, (3) c, and (4) d. Why do the diurnal variations of model-simulated Isoprene and its oxidation products MVK and MACR exhibit a bimodal distribution, which is opposite to the observed diurnal characteristics? Since isoprene is a typical biogenic VOC, it is reasonable for its concentration to be high during the daytime, while the model-simulated values are close to zero at noon.*
Response: The model bias in the noon peak of isoprene is likely attributed to the underestimation in biogenic emissions from urban green spaces, which further affects

the simulation of MVK and MACR. We have added a related discussion in the revised manuscript:

Lines 238-242: "Notably, biases in OVOC concentrations are influenced by those of their precursors. For example, model biases in methacrolein (MACR) and methyl vinyl ketone (MVK) exhibited similar temporal patterns to those of isoprene (ISOP), reflecting their common origin via isoprene oxidation. The model failed to reproduce the peak noon concentration of isoprene, likely due to the underestimated biogenic emissions from urban green spaces."

Comment: *9. Line 44. Delete "and thus deviate from observations".*

Response: The phrase has been removed.

References

Gao, Y., Wang, H., Yuan, L., Jing, S., Yuan, B., Shen, G., Zhu, L., Koss, A., Li, Y., Wang, Q., Huang, D. D., Zhu, S., Tao, S., Lou, S., and Huang, C.: Measurement report: Underestimated reactive organic gases from residential combustion – insights from a near-complete speciation, Atmos. Chem. Phys., 23, 6633-6646, 10.5194/acp-23-6633-2023, 2023.

Gao, Y. Q., Wang, H. L., Liu, Y., Zhang, X., Jing, S. A., Peng, Y. R., Huang, D. D., Li, X., Chen, S. Y., Lou, S. R., Li, Y. J., and Huang, C.: Unexpected High Contribution of Residential Biomass Burning to Non-Methane Organic Gases (NMOGs) in the Yangtze River Delta Region of China, J. Geophys. Res. Atmos., 127, 14, 10.1029/2021jd035050, 2022.

Pagonis, D., Sekimoto, K., and de Gouw, J.: A Library of Proton-Transfer Reactions of H3O+ Ions Used for Trace Gas Detection, Journal of the American Society for Mass Spectrometry, 30, 1330-1335, 10.1007/s13361-019-02209-3, 2019.

Qin, M. M., She, Y. L., Wang, M., Wang, H. L., Chang, Y. H., Tan, Z. F., An, J. Y., Huang, J., Yuan, Z. B., Lu, J., Wang, Q., Liu, C., Liu, Z. X., Xie, X. D., Li, J. Y., Liao, H., Pye, H. O. T., Huang, C., Guo, S., Hu, M., Zhang, Y. H., Jacob, D. J., and Hu, J. L.: Increased urban ozone in heatwaves due to temperature-induced emissions of anthropogenic volatile organic compounds, Nat. Geosci, 15, 10.1038/s41561-024-01608-w, 2025.

Sekimoto, K., Li, S.-M., Yuan, B., Koss, A., Coggon, M., Warneke, C., and de Gouw, J.: Calculation of the sensitivity of proton-transfer-reaction mass spectrometry (PTR-MS) for organic trace gases using molecular properties, International Journal of Mass Spectrometry, 421, 71-94, https://doi.org/10.1016/j.ijms.2017.04.006, 2017.